PFC/JA-96-34

Measurements of Neutral Density Based on H_α Emissivity in the Alcator C-Mod Divertor

C. Kurz, B. LaBombard, B. Lipschultz,
G. McCracken, A. Niemczewski, J. Terry

October 1996

Plasma Phys. and Controlled Fusion.

This work was supported by the U. S. Department of Energy Contract No. DE-AC02-78ET51013. Reproduction, translation, publication, use and disposal, in whole or in part by or for the United States government is permitted.

Measurements of Neutral Density Based on H_α Emissivity in the Alcator C-Mod Divertor

C. Kurz, B. LaBombard, B. Lipschultz,
G. McCracken, A. Niemczewski, J. Terry

May 6, 1996

Abstract

Neutral density profiles have been derived along the outboard divertor target of Alcator C-Mod and inside the last closed flux surface (LCFS). Local H_α emission rates are obtained by a tomographic inversion of measured H_α brightness profiles. Electron temperatures and densities provided by a divertor Langmuir probe array are then used to calculate the local neutral density, n_n, from the H_α emissivity profile. For points inside the LCFS, ECE and interferometry data were used for electron density and temperature, respectively. Along the divertor target, steep gradients in neutral density persist during regular ohmic attached discharges, with $n_n \approx 2 \times 10^{19}$ m^{-3}. Plasma detachment leads to values of n_n that can reach up to several times 10^{20} m^{-3} in the bottom of the divertor with much shallower pressure gradients to the midplane. Modelling of the parallel plasma momentum decrease due to charge exchange (CX) indicates that neutral densities between one and two orders of magnitude below the values observed are sufficient to explain the measured drop in parallel plasma pressure. This suggests that significant momentum is carried by the neutrals in the divertor resulting in decreased efficiency of momentum transfer between ions and neutrals.

1 Introduction

An important goal of current plasma edge research is the reduction of heat and particle fluxes to the material surfaces at the divertor target. The physics issues central to this goal are power and pressure balance in the plasma edge region, which, in turn, are governed by radiation and charge

exchange (CX). It is well known that high density operation with its associated lower temperature maximizes radiation in the Scrape-off-Layer (SOL) near the divertor and leads to a regime where the plasma detaches locally from the divertor target. There exists experimental as well as theoretical evidence that plasma-neutral interactions play a major role in the momentum and power balances during these conditions [1]. These interactions directly affect the power radiated by hydrogen and impurities, and result in momentum transfer from the ion-fluid to the neutrals through CX and other ion-neutral interactions. For these reasons the neutral density has also been found to be an important factor in the achievement of plasma detachment [1].

The emission rate of H_α photons is governed by Equ. 1:

$$S_\alpha = n_e n_n \langle \sigma v \rangle_{\alpha x}, \tag{1}$$

where S_α is the H_α photon emissivity (H_α photons/m^3 s), n_e and n_n are the electron and neutral densities respectively, and $\langle \sigma v \rangle_{\alpha x}$ is the H_α excitation rate coefficient which depends on n_e and T_e. The neutral density is then obtained from Equ. 1:

$$n_n = \frac{S_\alpha}{n_e \langle \sigma v \rangle_{\alpha x}}. \tag{2}$$

Numerical values for $\langle \sigma v \rangle_{\alpha x}$ were calculated using the formalism described by Johnson and Hinnov [2]. For temperatures $T_e \leq 4$ eV the dependence of $\langle \sigma v \rangle_{\alpha x}$ on T_e is so strong that the corresponding uncertainty in n_n becomes excessive (± 1 eV results in a factor of 10 difference in $\langle \sigma v \rangle_{\alpha x}$). Since the temperature in the private flux zone is frequently below 4 eV, values of n_n from this region are fraught with large errors and are not quoted in this paper.

2 Experimental Technique

Alcator C-Mod is equipped with an optical imaging system providing comprehensive coverage of the entire poloidal cross section (see Fig. 1). Four filtered views, each comprising 64 absolutely calibrated detectors, provide sufficient information to allow a tomographic inversion of the measured H_α brightness data. A description of this system can be found in Ref. [3]. The tomographic inversion employs a non-linearly constrained least-squares algorithm with spatial smoothing on a discrete pixel grid. A previous version of this method has been published in Ref. [4]; significant improvements have

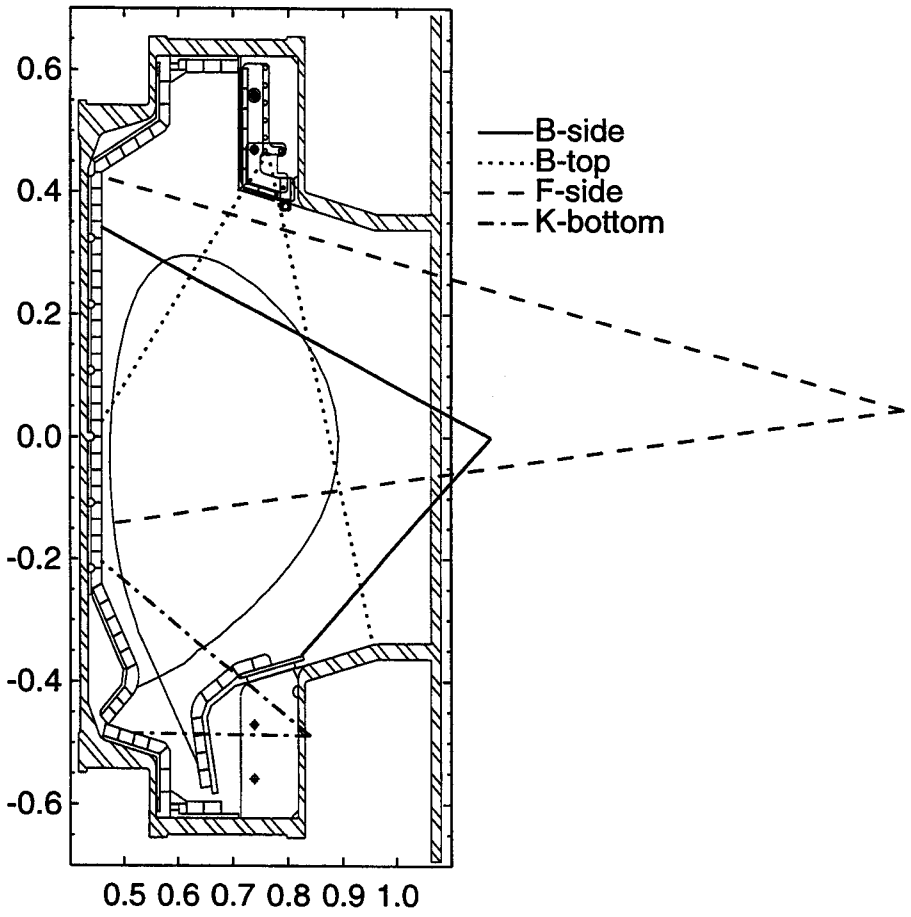

Figure 1: The imaging system has four views of the plasma, each comprising 64 individual chords, covering the entire light emitting region. Note that the arrays are not collocated toroidally.

been made in the present analysis, resulting in a spatial resolution of 2.5 cm [5]. To facilitate plotting and contouring of the data, the calculated H_α emission profiles have been linearly interpolated onto a finer spatial grid, except where otherwise noted. This technique calculates the H_α emissivity assuming toroidal symmetry of the emission but with no assumptions regarding the poloidal distribution.

Fig. 2 shows a close-up of the Alcator C-Mod divertor region indicating the location of the Langmuir probes in the divertor target (10 probes along the outboard and 6 probes along the inboard side). In addition to the

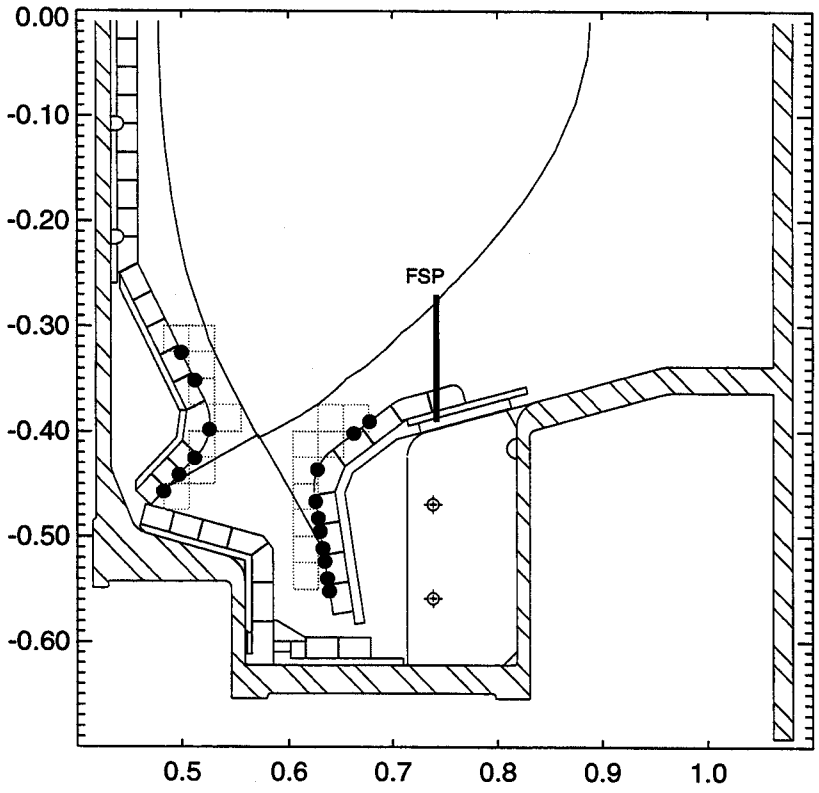

Figure 2: The Alcator C-Mod divertor showing the location of Langmuir probes embedded in the inner and outer divertor targets (full circles) and the Fast Scanning Probe (FSP). Also shown are the locations of pixels along the outboard divertor from which the emissivity was used to calculate the neutral density.

Langmuir probes in the divertor, there is also a Fast Scanning Probe (FSP)

upstream of the outboard divertor. It is pneumatically actuated and is capable of measuring n_e and T_e profiles across the entire width of the SOL up to three times per discharge. Also shown in Fig. 2 are the locations of pixels adjacent to the divertor surface. Emissivity values in these pixels have been used, together with temperature and density data from adjacent probes, to calculate the neutral density at the probe locations using Equ. 2 (assuming no contribution from molecular deuterium). Experimental measurements of the neutral molecular density have been made at the torus midplane and under the outboard divertor target with a fast ionization gauge [6, 7]. The neutral molecular density measured in this way will be compared with the neutral atomic densities derived from the H_α data.

3 Neutral Density Measurements

A series of ohmically heated discharges at $B_t = 5.3$ T with increasing densities have been examined. Their global parameters are summarized in Tab. 1. Increasing $\bar{n}_e$ from shot to shot (see Tab. 1) leads to local plasma detachment

Shot	Time (s)	I_p (kA)	$\bar{n}_e(10^{20}$ m$^{-3})$	P_{OH} (kW)	P_{SOL} (kW)
950202006	0.683	822	1.2	949	607
950202007	0.683	816	1.5	938	633
950202010	0.684	810	1.9	1205	638
950202011	0.684	806	2.2	1230	567
950202013	0.685	806	2.5	1287	536

Table 1: Global parameters for the sequence of shots used in the neutral density calculation. P_{OH} is the ohmic input power, P_{SOL} is the power crossing the LCFS.

in the divertor, which reaches progressively farther radially outward into the SOL. A comparison of the upstream (measured by the FSP) plasma pressure to its value at the target is shown in Fig. 3 for three of the five discharges.

In the following discussion field lines are labeled by ρ, their distance from the separatrix measured at the midplane. A positive value for ρ indicates positions outside of the separatrix, in the common flux region. Field lines inside the separatrix have $\rho > 0$. Note that, topologically, positions in the private flux region below the X point are also labeled by positive values for ρ.

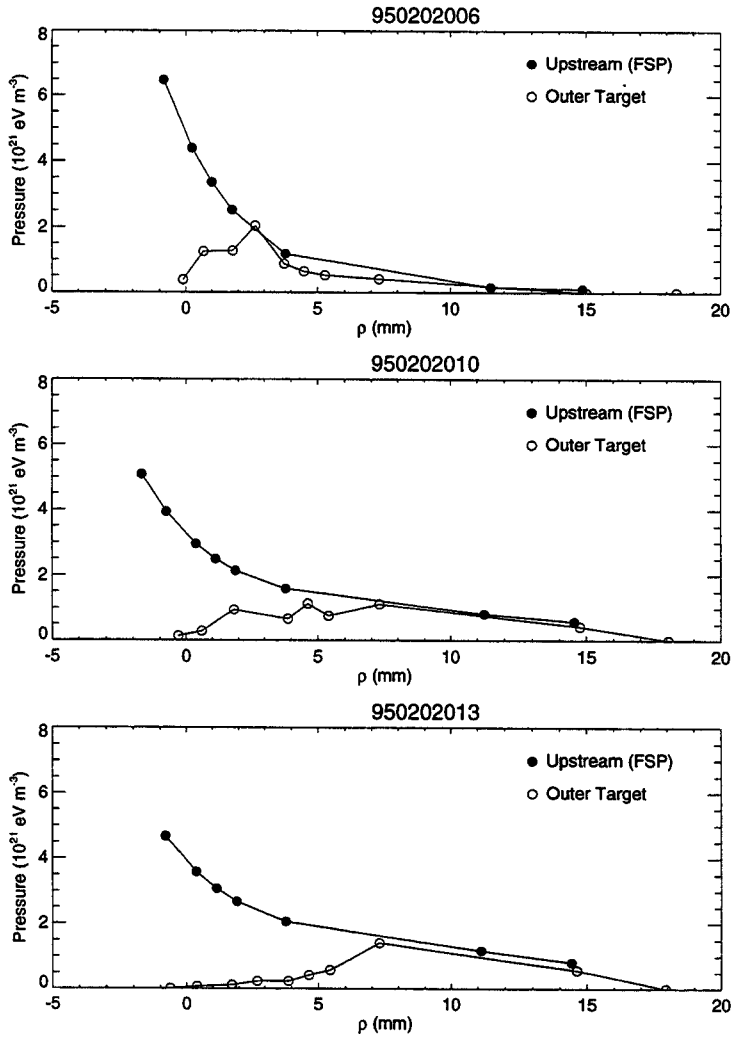

Figure 3: Comparison of the upstream and downstream plasma pressure for three discharges listed in Tab. 1. The horizontal coordinate ρ measures the distance of a flux line outside of the separatrix, mapped to the midplane (negative values stand for the region inside the separatrix (FSP) or the private flux region (divertor probes). Increasing degrees of detachment are indicated by the extent of the region over which upstream and downstream measurements do not map.

Shot 950202006 is typical of a mostly attached plasma condition indicated by the accurate mapping of plasma pressure for $\rho \geq 2$ mm. At the other extreme, shot 950202013 is representative of a deeply detached plasma condition as shown by the pressure drop which reaches out to $\rho = 7$ mm. Shot 950202010 falls somewhere in the middle.

The H_α emission profile in the divertor undergoes a rearrangement during detachment. For most attached shots the H_α emission is dominated by a well localized bright region just above the inboard divertor nose (see Fig. 4). The position of this bright feature is confirmed by images from video

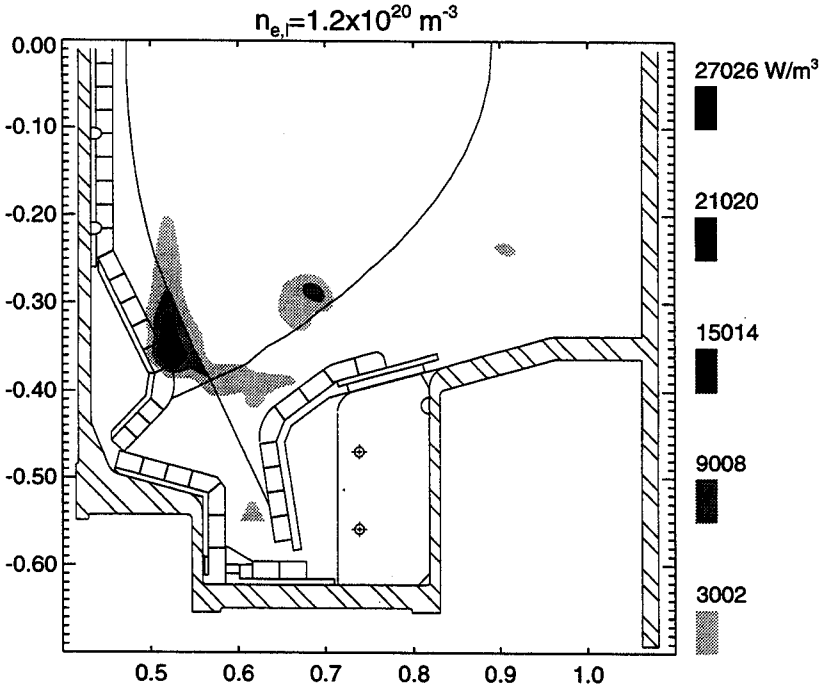

Figure 4: H_α emission from shot 950202006, at $t = 0.683$ s. The emission is dominated by a bright, localized region just above the inboard divertor nose. This is typical for attached divertor plasma conditions.

cameras, viewing the plasma tangential to the major radius. It is present also when viewed at various wavelengths of CII and CIII emission. Comparatively little visible radiation comes from the divertor region or from parts above the midplane.

In the case of a deep detachment (950202013), the emission has increased significantly and is smeared out over a much larger area which extends from

above the inner divertor nose down into the bottom of the divertor (see Fig. 5), following predominantly the outer leg of the separatrix. We also observe that the amount of H_α radiation from inside the LCFS is larger than in the attached case.

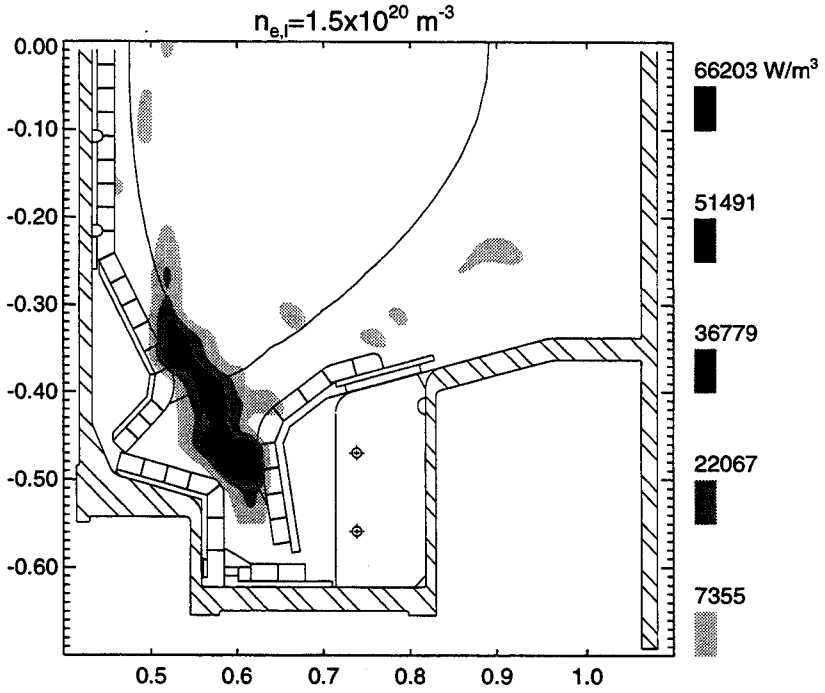

Figure 5: H_α emission from shot 950202013, at $t = 0.685$ s, during deeply detached divertor plasma conditions. Notice the increased emission over the case shown in the previous figure. Significant H_α light comes from the bottom parts of the divertor and extends along the outer separatrix leg up to above the inboard nose.

It is in principle possible to deduce neutral densities for locations inside the LCFS using electron density and temperature information from interferometry and ECE, respectively. Since, however, the emission of H_α light changes sharply over distances measured in millimeters just inside the LCFS, the size of the inversion grid poses a severe limitation in this region. To show the quality of information obtainable from tomography, the top panel of Fig. 6 is a plot of the H_α reconstruction for an attached discharge. The bottom panel is the result of a neutral density calculation using Equ. 2. Electron density and temperature outside the LCFS are based on Langmuir probe measurements interpolated between divertor probes and the FSP using a

simple one-dimensional conduction model [5, 8].

Because of the sensitive dependence of the H_α excitation rate coefficient on T_e, only pixels adjacent to the probe arrays have been considered in the following analysis. For these pixels the temperature and density were taken directly from the adjacent Langmuir probe array. The accurate calculation of neutral density profiles away from the regions where direct measurements of T_e and n_e are available is in principle possible but requires a reliable computer model of the SOL conditions, particularly in the low temperature region of the private flux zone.

A neutral density profile along the divertor target plates was calculated in this manner for all five discharges listed in Tab. 1. Fig. 7 summarizes the results of these calculations. Unfortunately, the temperature at the inboard divertor plate was generally too low to permit a meaningful calculation of n_n without accumulating excessive errors. Only three data points (open circles) are shown for the inboard side; they correspond to shot 950202011. The inboard neutral density in these cases is only slightly higher than the corresponding outboard density. However, in general it is observed from probe measurements that the electron density is significantly higher inboard and the temperature lower than at corresponding locations on the outboard target.

The neutral atomic density obtained from the H_α measurements has been compared to the molecular density measured with a fast linear ionization gauge installed outside the plasma behind the outboard divertor target and another gauge at the outboard midplane. In order to compare data from gauges outside the plasma region with the atomic density at the target, the following assumptions have been made:

- The energy of the atomic neutrals is 3 eV, determined by Franck-Condon dissociation.
- Particle flux conservation holds across the plasma boundary.

The neutral density spans about three orders of magnitude across the set of discharges ("a" – "e"). The divertor neutral pressure is a strong function of the line integrated plasma density in the main plasma; this behavior has been documented before [9]

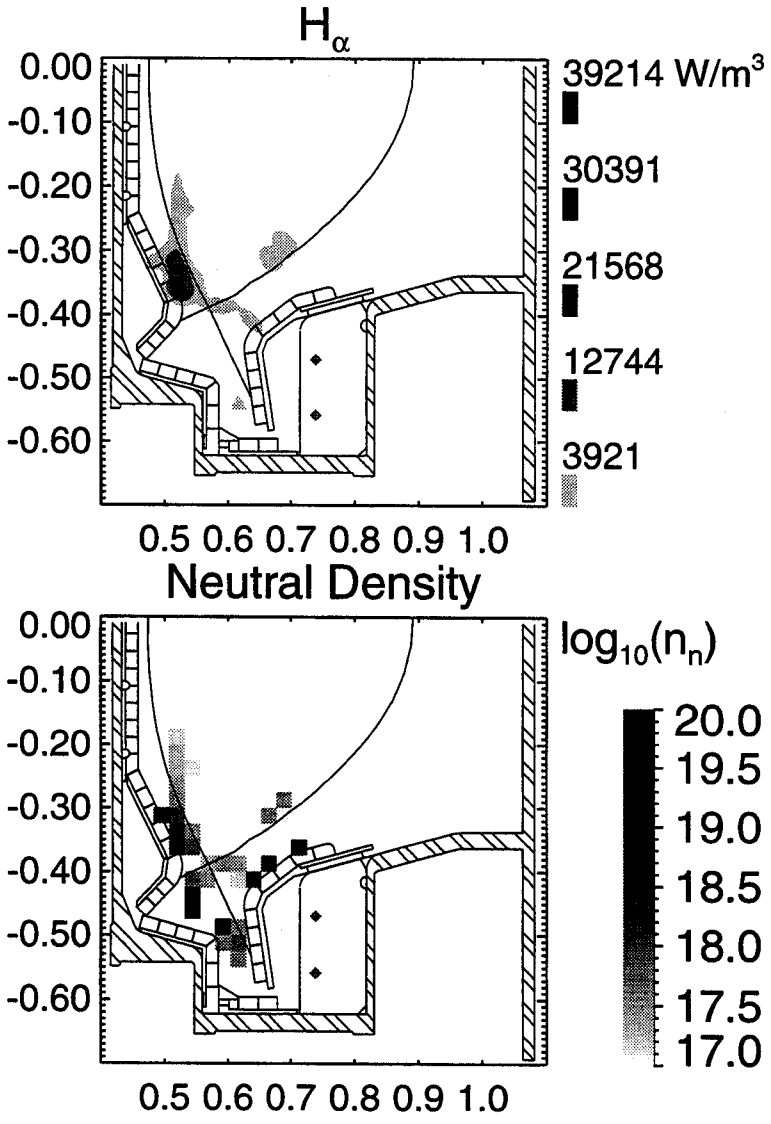

Figure 6: Top: H_α emissivity obtained by tomographic reconstruction, for an attached discharge with $\bar{n}_e = 1.2 \times 10^{20}$ m^{-3}. Bottom: neutral density calculated from reconstructed emissivity shown above. Profiles for n_e and T_e outside te LCFS are obtained from a 1D conduction model. For the low temperatures in the private flux region, where n_e and T_e values are unreliable, the neutral density is only correct to order of magnitude.

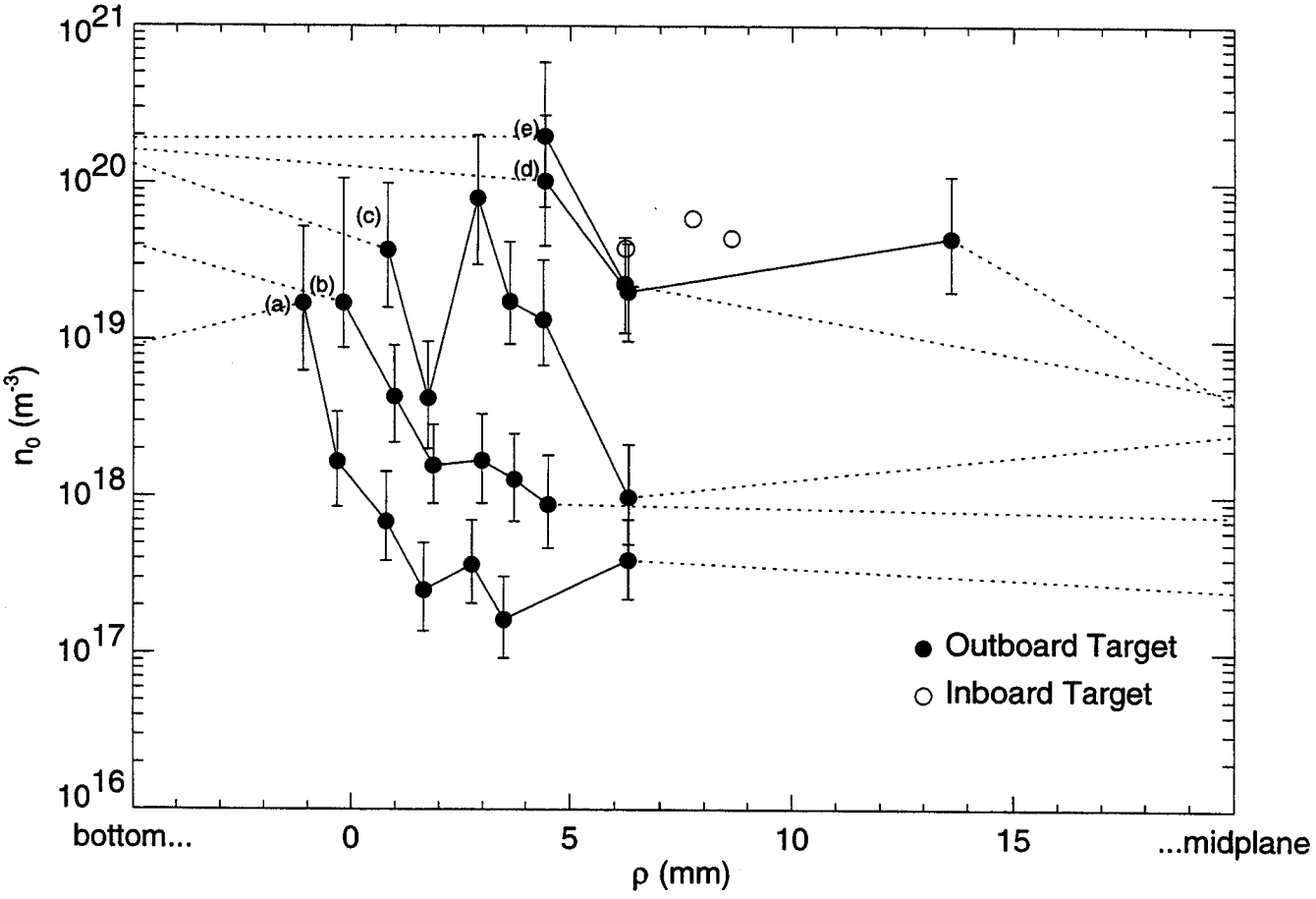

Figure 7: Neutral density profiles along the outboard divertor target for the five discharges listed in Tab. 1 (a:950202006, b:950202007, c:950202010, d:950202011, e:950202013); three data points are shown for the inboard divertor for shot 950202011. The dotted lines leading to the right connect the last calculated point with the corresponding measurement of a neutral pressure gauge at the midplane. The dotted lines on the left connect the first calculated point to the neutral measurement of a pressure gauge installed at the bottom of the divertor.

4 Discussion

The neutral density and pressure differential between the private flux zone and the midplane can be very high for low density discharges (traces "a" and "b"); a pressure drop of two orders of magnitude is sustained over a distance of 7 mm in the radial coordinate ρ, corresponding to a distance of approximately 10 cm in real space. At higher densities ("d" and "e") the neutral density profile flattens out considerably; it drops by roughly one order of magnitude between the private flux zone and a point at $\rho = 15$ mm. This constitutes a change in the neutral density gradient by a factor of 20. A significantly higher midplane neutral pressure occurs during detached divertor discharges.

The difference in parallel plasma momentum between upstream and downstream measurements (c.f. Fig. 3) is characteristic of plasma detachment. Ion-neutral interactions in the cold region close to the target plate participate in the momentum balance when CX events become the dominant ion-neutral interaction. This is reflected in the momentum balance equation:

$$\frac{dp}{ds} = m_i n_n \Gamma \langle \sigma v \rangle_{cx} . \tag{3}$$

In Equ. 3, s measures the distance along the field line, m_i is the ion mass, and Γ the particle flux. The neutral density required to produce a certain drop in pressure can then be estimated from Equ. 3:

$$n_n \approx \frac{\Delta p}{\Delta s} \frac{1}{m_i \Gamma \langle \sigma v \rangle_{cx}} . \tag{4}$$

The quantity Δs is the width of the region (measured along a field line) over which CX dominates ion-neutral interactions. For simplicity's sake, this has been taken as the distance from the target plate to the point where $T = 6$ eV. The location at which the temperature reaches 6 eV is estimated from a 1-D conduction model including localized radiation and heating [8] in a single fluid description (i.e. $T_i = T_e$). The neutral density calculated is not very sensitive to T_i since $\langle \sigma v \rangle$ is approximately constant with temperature. Tab. 2 compares n_n derived from H_α measurements (from Fig. 7) and calculated from Equ. 4 for $\rho = 1$ mm across the set of discharges listed in Tab. 1. In the high-recycling regime (shots 950202006 and 950202007) the neutral densities inferred from the pressure drop (third column in Tab. 2) and the H_α emission (fourth column) agree within experimental errors. This changes when considering higher density detached shots (Tab. 2). Here the calculated

Shot	Time (s)	n_n(m^{-3}) from model	n_n(m^{-3}) from H_α data	H_α /model
950202006	0.683	1.5×10^{18}	6×10^{17}	2.5
950202007	0.683	9.7×10^{18}	4×10^{18}	2.4
950202010	0.684	5.6×10^{18}	5×10^{19}	0.11
950202011	0.684	5.8×10^{18}	1.5×10^{20}	0.04
950202013	0.685	6.1×10^{18}	2.5×10^{20}	0.02

Table 2: Comparison of neutral density calculated from the plasma pressure drop along a field line to the experimental result from Fig. 7. The ratio of the neutral densities from H_α measurement to the one derived by Equ. 4 is entered in the last column.

neutral density varies little with $\bar{n}_e$ and is roughly 10 to 50 times lower than the experimental value. The difference increases with $\bar{n}_e$ from shot 950202010 to 950202013. It appears as if ion-neutral collisions are not as effective as predicted by Equ. 3 in dissipating plasma ion momentum at high densities.

Application of Equ. 4 implicitly assumes stationary neutrals which completely remove the acquired ion momentum from the plasma after one collision. However, if a neutral has successive ion-neutral interactions after the first one, it is not expected to remove significant plasma ion momentum until the neutral has lost its momentum through, e.g., contact with the wall. At a Franck-Condon energy of 3 eV, a plasma temperature of 5 eV and a plasma density of 10^{20} m^{-3}, the CX mean-free-path, λ_{cx}, is 9 mm. Given the Alcator C-Mod divertor geometry (c.f. Fig. 2, a neutral may be an average distance of 5 cm from a divertor surface and therefore may undergo 5 CX collisions prior to contacting the wall. Therefore, an initially stationary neutral is maybe about 20% effective in transferring momentum from the plasma to the divertor. This effect is of the right magnitude to reconcile the observed neutral densities with the measured plasma pressure drop. A consequence of this is that, at high densities, the neutrals have a velocity comparable to the bulk plasma flow, thus reducing the efficiency of momentum removal even further.

5 Conclusion

We have used H_α emissivity profiles calculated by a tomographic inversion algorithm together with Langmuir probe data to calculate the neutral den-

sity. These calculation have yielded neutral density profiles along the outboard divertor target, which are in good agreement with data from neutral pressure gauges installed at the midplane and the bottom of the divertor. The measured neutral densities during detached divertor plasma conditions are significantly higher (by a factor of 20 – 50) than needed to explain the observed decrease in plasma momentum between the target and a probe upstream through CX interactions. The bulk flow of neutrals suggested by this observation is a focus of ongoing work.

References

[1] P. C. Stangeby. *Nuc. Fus.*, 33(11):1695, 1993.

[2] L. C. Johnson and E. Hinnov. *J. Quant. Spect. Radiat. Trans.*, 13:333, 1973.

[3] J. L. Terry, J. A. Snipes, and C. Kurz. *Rev. Sci. Instrum.*, 66(1):555, January 1995.

[4] C. Kurz, J. A. Snipes, J. L. Terry, B. Labombard, B. Lipschultz, and G. M. McCracken. *Rev. Sci. Instrum.*, 66(1):619 – 621, January 1995.

[5] C. Kurz. *Tomography of light emission from the plasma edge of Alcator C-Mod.* PhD thesis, Massachusetts Institute of Technology, 1995.

[6] A. Niemczewski, B. Lipschultz, B. LaBombard, and G. M. McCracken. In-situ neutral pressure measurements in a compact high-field tokamak, Alcator C-Mod. *Rev. Sci. Instrum.*, January 1995. (To be published).

[7] A. Niemczewski. PhD thesis, Massachusetts Institute of Technology, 1995.

[8] J. Kesner. Detached scrape-off layer tokamak plasmas. (Submitted to Physics of Plasmas).

[9] A. Niemczewski, B. LaBombard, B. Lipschultz, and G. M. McCracken. Technical Report PFC/RR-94-13, M.I.T.,Plasm Fusion Center, November 1994.